

## Two-loop corrections to polarized $\gamma\gamma \rightarrow \gamma\gamma$ process

S. Bondarenko<sup>1,4</sup>, A. Issadykov<sup>1,3</sup>, L.V. Kalinovskaya<sup>2,5</sup>, A.A. Sapronov<sup>2</sup>,  
D. Seitova<sup>3</sup>

<sup>1</sup> BLTP JINR, Dubna, Russia

<sup>2</sup> DLNP JINR, Dubna, Russia

<sup>3</sup> INP ME of RK, Almaty, Kazakhstan

<sup>4</sup> DSU, Dubna, Russia

<sup>5</sup> LSU, Moscow, Russia

**The International Conference Mathematical Modeling and  
Computational Physics, 2024 (MMCP2024),  
20–25 Oct 2024, Yerevan, Armenia**

## Motivation

Growing interest to photon-photon collider physics in the scientific community:

- Higgs physics
- SM benchmarks
- New physics (SUSY)
- QCD tests (photon structure function, jet production)
- Flavor physics ( $\eta_c$ )

The gamma-gamma collisions may constitute significant background for e+e-colliders (equivalent photons, beamstrahlung)

Our study was initiated by our colleagues from Novosibirsk

Table 3. Gold-plated processes at photon colliders.

Reaction	Remarks
$\gamma\gamma \rightarrow h^0 \rightarrow b\bar{b}$	SM (or MSSM) Higgs, $M_{h^0} < 160$ GeV
$\gamma\gamma \rightarrow h^0 \rightarrow WW(WW^*)$	SM Higgs, $140 \text{ GeV} < M_{h^0} < 190$ GeV
$\gamma\gamma \rightarrow h^0 \rightarrow ZZ(ZZ^*)$	SM Higgs, $180 \text{ GeV} < M_{h^0} < 350$ GeV
$\gamma\gamma \rightarrow H, A \rightarrow b\bar{b}$	MSSM heavy Higgs, for intermediate $\tan\beta$
$\gamma\gamma \rightarrow \tilde{f}\tilde{f}^*, \tilde{\chi}_i^+ \tilde{\chi}_i^-, H^+ H^-$	large cross-sections, possible observations of FCNC
$\gamma\gamma \rightarrow S[\tilde{t}\tilde{t}^*]$	$\tilde{t}\tilde{t}^*$ stoponium
$\gamma e \rightarrow \tilde{e}^- \tilde{\chi}_1^0$	$M_{\tilde{e}^-} < 0.9 \times 2E_0 - M_{\tilde{\chi}_1^0}$
$\gamma\gamma \rightarrow W^+ W^-$	anomalous $W$ interactions, extra dimensions
$\gamma e^- \rightarrow W^- \nu_e$	anomalous $W$ couplings
$\gamma\gamma \rightarrow WWWW, WWZZ$	strong $WW$ scatt., quartic anomalous $W, Z$ couplings
$\gamma\gamma \rightarrow t\bar{t}$	anomalous top quark interactions
$\gamma e^- \rightarrow \bar{t} b \nu_e$	anomalous $Wtb$ coupling
$\gamma\gamma \rightarrow \text{hadrons}$	total $\gamma\gamma$ cross-section
$\gamma e^- \rightarrow e^- X$ and $\nu_e X$	$\mathcal{N}C$ and $CC$ structure functions (polarized and unpolarized)
$\gamma g \rightarrow q\bar{q}, c\bar{c}$	gluon distribution in the photon
$\gamma\gamma \rightarrow J/\psi, \psi, \psi$	QCD Pomeron

(taken from [Boos et.al. Nucl.Instrum.Meth.A472:100-120,2001])

## Photon-photon collisions in SANC

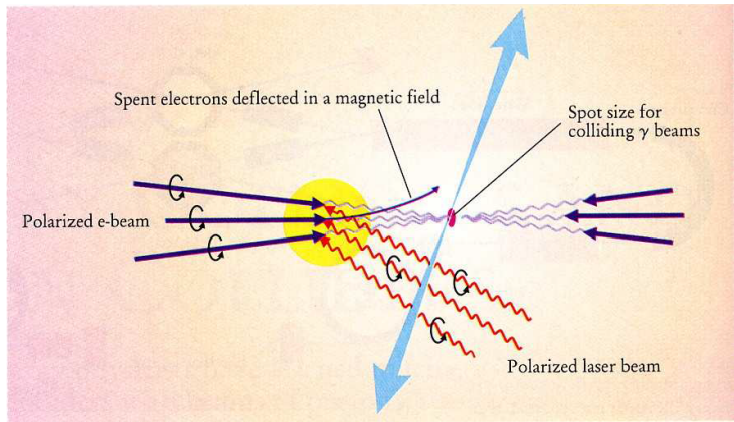
The unpolarized  $\gamma\gamma \rightarrow \gamma\gamma, Z\gamma, ZZ$  SM processes through fermion and boson loops were calculated within the SANC framework by D. Bardin, S. Bondarenko, L. Kalinovskaya and E. Uglov.

The computations take into account non-zero mass of loop particles and massive box diagrams.

The results are presented as the covariant and helicity amplitudes for these processes with some particular cases of D0 and C0 Passarino-Veltman functions.  
Reference: Phys.Atom.Nucl.73:1878-1888,2010

The form of helicity amplitudes allows to implement the same calculations taking into account the photon polarizations.

## Polarized gamma beams at e+e- collider



(picture taken from slides of V.Serbo "Basics of photon collider" )

## Polarized gamma-gamma cross section

The differential photon-photon cross section taking into account polarizations can be taken from [Gounaris et.al. Eur.Phys.J.C10:499-513,1999]:

$$\begin{aligned} \frac{d\sigma}{d\tau d\cos\vartheta^*} = & \frac{d\bar{L}_{\gamma\gamma}}{d\tau} \left\{ \frac{d\bar{\sigma}_0}{d\cos\vartheta^*} + \langle \xi_2 \xi_2' \rangle \frac{d\bar{\sigma}_{22}}{d\cos\vartheta^*} + \langle \xi_3 \rangle \cos 2\phi \frac{d\bar{\sigma}_3}{d\cos\vartheta^*} + \langle \xi_3' \rangle \cos 2\phi' \frac{d\bar{\sigma}'_3}{d\cos\vartheta^*} \right. \\ & + \langle \xi_3 \xi_3' \rangle \left[ \frac{d\bar{\sigma}_{33}}{d\cos\vartheta^*} \cos 2(\phi + \phi') + \frac{d\bar{\sigma}'_{33}}{d\cos\vartheta^*} \cos 2(\phi - \phi') \right] \\ & \left. + \langle \xi_2 \xi_3' \rangle \sin 2\phi' \frac{d\bar{\sigma}_{23}}{d\cos\vartheta^*} - \langle \xi_3 \xi_2' \rangle \sin 2\phi \frac{d\bar{\sigma}'_{23}}{d\cos\vartheta^*} \right\}, \end{aligned} \quad (10)$$

factor  $dL_{\gamma\gamma}/d\tau$  – the photon-photon luminosity per unit  $e^+e^-$ ,  $\theta^*$  – the  $\gamma\gamma$  collision products scattering angle in the incoming particles rest frame, the  $\tau = s_{\gamma\gamma}/s_{ee}$  – fraction of electron beams energy transferred to the colliding photons,  $k_{si}$  – Stock's parameters.

## Polarized gamma-gamma cross section

$$\frac{d\bar{\sigma}_0}{d\cos\vartheta^*} = N \sum_{\lambda_3\lambda_4} [|\mathcal{H}_{++\lambda_3\lambda_4}|^2 + |\mathcal{H}_{+-\lambda_3\lambda_4}|^2]$$

$$\frac{d\bar{\sigma}_{22}}{d\cos\vartheta^*} = N \sum_{\lambda_3\lambda_4} [|\mathcal{H}_{++\lambda_3\lambda_4}|^2 - |\mathcal{H}_{+-\lambda_3\lambda_4}|^2]$$

$$\frac{d\bar{\sigma}_3}{d\cos\vartheta^*} = -2N \sum_{\lambda_3\lambda_4} \text{Re} [\mathcal{H}_{++\lambda_3\lambda_4} \mathcal{H}_{-+\lambda_3\lambda_4}^*]$$

$$\frac{d\bar{\sigma}'_3}{d\cos\vartheta^*} = -2N \sum_{\lambda_3\lambda_4} \text{Re} [\mathcal{H}_{++\lambda_3\lambda_4} \mathcal{H}_{--\lambda_3\lambda_4}^*]$$

$$\frac{d\bar{\sigma}_{33}}{d\cos\vartheta^*} = N \sum_{\lambda_3\lambda_4} \text{Re} [\mathcal{H}_{++\lambda_3\lambda_4} \mathcal{H}_{--\lambda_3\lambda_4}^*]$$

$$\frac{d\bar{\sigma}'_{33}}{d\cos\vartheta^*} = N \sum_{\lambda_3\lambda_4} \text{Re} [\mathcal{H}_{++\lambda_3\lambda_4} \mathcal{H}_{--\lambda_3\lambda_4}^*]$$

$$\frac{d\bar{\sigma}_{23}}{d\cos\vartheta^*} = 2N \sum_{\lambda_3\lambda_4} \text{Im} [\mathcal{H}_{++\lambda_3\lambda_4} \mathcal{H}_{+-\lambda_3\lambda_4}^*], \text{ where } N = \frac{\beta_z}{64\pi\hat{s}}$$

## Density matrix

After a Compton scattering of  $e^\pm$  off a laser photon, the electron (positron) beam loses most of its energy and a beam of "backscattered photons" is produced, moving essentially along the direction of the original  $e^\pm$  momentum and characterized, in its helicity basis, by the density matrix:

$$\rho^{BN} = \frac{1}{2} \begin{pmatrix} 1 + \xi_2(x) & -\xi_3(x)e^{-2i\phi} \\ -\xi_3(x)e^{+2i\phi} & 1 - \xi_2(x) \end{pmatrix}$$

where  $x = \omega/E$  is the back-scattered photon energy fraction.

$$\xi = \xi(P_e, P_\gamma, P_t),$$

where  $P_e = 2\lambda_e$  – electron/positron longitudinal polarization, and  $\lambda_e$  is its average helicity,  $P_\gamma$  – the average helicity of the laser photon,  $P_t$  ( $P_t \geq 0$ ) – maximum average transverse polarization along a direction determined by the azimuthal angle  $\phi$ .



## 1-loop $\gamma\gamma$ scattering in SANC: SANCphot v1.01

We reuse the MCSANC code to create a stand-alone SANCphot package to implement the  $\gamma\gamma \rightarrow \gamma\gamma, Z\gamma$ , and  $ZZ$  processes relying on the Fortran modules created within the SANC framework at 1-loop level (LO).

The Monte-Carlo calculation requires:

- Initial electron beam energy, laser energy
- Laser and electron polarizations, with laser polarization could be both longitudinal and transverse
- Final Z particle polarization

And the integration variables are:

- $\cos\theta^*$  — cosine of the final particle azimuthal angle
- $\tau = \frac{s_{\gamma\gamma}}{s_{ee}}$
- $x = \omega/E$

[1] S. Bondarenko, L. Kalinovskaya, A. Saprnov,  
Comput.Phys.Commun. 294 (2024) 108929; e-Print: 2201.04350  
[hep-ph]

## QCD- and QED-corrected 2-loop contributions

The QCD- and QED-corrected 2-loop amplitudes are given by the expressions:

$$\mathcal{H}_{\lambda_1 \lambda_2 \lambda_3 \lambda_4}^{2\text{-loop, QCD(QED)}} = N^{\text{QCD(QED)}} \mathcal{H}_{\lambda_1 \lambda_2 \lambda_3 \lambda_4}^{(2)}$$

with the coefficients  $N^{\text{QCD}} = 4(N^2 - 1)Q^4 \alpha^2 \frac{\alpha_s(M_z^2)}{\pi}$ , and

$N^{\text{QED}} = 8NQ^6 \alpha^2 \frac{\alpha(0)}{\pi}$ , where  $N$  is the fermion color factor (3 for quarks, 1 for leptons), and  $Q$  is the fermion charge in units of  $e$ .

$\mathcal{H}_{\lambda_1 \lambda_2 \lambda_3 \lambda_4}^{(2)}$  – 2-loop helicity amplitudes

## QCD- and QED-corrected 2-loop contributions

The expressions for the helicity amplitudes  $\mathcal{H}^{(2)}$  in the  $m_f = 0$  limit (where  $m_f$  is the fermion mass in a loop) are given in [2].

In the practical calculations, the top-quark contribution was taken into account for energies  $\sqrt{s} > 2m_t$ .

The helicity amplitudes in this case are:

$$\mathcal{H} = \mathcal{H}^{1\text{-loop}} + \mathcal{H}^{2\text{-loop, QCD(QED)}}.$$

In the calculations, the square of the  $\mathcal{H}^{2\text{-loop}}$  amplitude was omitted as part of the higher-order (3-loops) corrections.

[2] Z. Bern, A. De Freitas, L. J. Dixon, A. Ghinculov, and H. L. Wong, JHEP 11 (2001) 031, hep-ph/0109079

## Helicity amplitudes $\mathcal{H}^{(2)}$

$$M_{- - + +}^{(2)} = -\frac{3}{2}, \quad (\text{A.1})$$

$$M_{- + + +}^{(2)} = \frac{1}{8} \left[ \frac{x^2 + 1}{y^2} ((X + i\pi)^2 + \pi^2) + \frac{1}{2} (x^2 + y^2) ((X - Y)^2 + \pi^2) - 4 \left( \frac{1}{y} - x \right) (X + i\pi) \right] + \{t \leftrightarrow u\}, \quad (\text{A.2})$$

$$\begin{aligned} M_{+ + + +}^{(2)} = & -2x^2 \left[ \text{Li}_4(-x) + \text{Li}_4(-y) - (X + i\pi) (\text{Li}_3(-x) + \text{Li}_3(-y)) \right. \\ & \left. + \frac{1}{12} X^4 - \frac{1}{3} X^3 Y + \frac{\pi^2}{12} XY - \frac{4}{90} \pi^4 + i \frac{\pi}{6} X (X^2 - 3XY + \pi^2) \right] \\ & - (x - y) \left( \text{Li}_4(-x/y) - \frac{\pi^2}{6} \text{Li}_2(-x) \right) \\ & - x \left[ 2\text{Li}_3(-x) - \text{Li}_3(-x/y) - 3\zeta_3 - 2(X + i\pi) \text{Li}_2(-x) \right. \\ & \left. + (X - Y) (\text{Li}_2(-x/y) + X^2) + \frac{1}{12} (5(X - Y) + 18i\pi) ((X - Y)^2 + \pi^2) \right. \\ & \left. - \frac{2}{3} X (X^2 + \pi^2) - i\pi (Y^2 + \pi^2) \right] \\ & + \frac{1}{4} \frac{1 - 2x^2}{y^2} ((X + i\pi)^2 + \pi^2) - \frac{1}{8} (2xy + 3) ((X - Y)^2 + \pi^2) + \frac{\pi^2}{12} \\ & + \left( \frac{1}{2y} + x \right) (X + i\pi) - \frac{1}{4} + \{t \leftrightarrow u\}, \quad (\text{A.3}) \end{aligned}$$

## Helicity amplitudes $\mathcal{H}^{(2)}$

$$\begin{aligned} M_{+--+}^{(2)} = & -2\frac{x^2+1}{y^2} \left[ \text{Li}_4(-x/y) - \text{Li}_4(-y) + \frac{1}{2}(X-2Y-i\pi)(\text{Li}_3(-x) - \zeta_3) \right. \\ & \left. + \frac{1}{24}(X^4 + 2i\pi X^3 - 4XY^3 + Y^4 + 2\pi^2 Y^2) + \frac{7}{360}\pi^4 \right] \\ & - 2\frac{x-1}{y} \left[ \text{Li}_4(-x) - \zeta_4 - \frac{1}{2}(X+i\pi)(\text{Li}_3(-x) - \zeta_3) \right. \\ & \left. + \frac{\pi^2}{6}(\text{Li}_2(-x) - \frac{\pi^2}{6} - \frac{1}{2}X^2) - \frac{1}{48}X^4 \right] \\ & + \left(2\frac{x}{y} - 1\right) \left[ \text{Li}_3(-x) - (X+i\pi)\text{Li}_2(-x) + \zeta_3 - \frac{1}{6}X^3 - \frac{\pi^2}{3}(X+Y) \right. \\ & \left. + 2\left(2\frac{x}{y} + 1\right) \left[ \text{Li}_3(-y) + (Y+i\pi)\text{Li}_2(-x) - \zeta_3 + \frac{1}{4}X(2Y^2 + \pi^2) \right. \right. \\ & \left. \left. - \frac{1}{8}X^2(X+3i\pi) \right] - \frac{1}{4}(2x^2 - y^2)((X-Y)^2 + \pi^2) \right. \\ & \left. - \frac{1}{4}\left(3 + 2\frac{x}{y^2}\right)((X+i\pi)^2 + \pi^2) - \frac{2-y^2}{4x^2}((Y+i\pi)^2 + \pi^2) + \frac{\pi^2}{6} \right. \\ & \left. + \frac{1}{2}(2x+y^2) \left[ \frac{1}{y}(X+i\pi) + \frac{1}{x}(Y+i\pi) \right] - \frac{1}{2}. \right. \end{aligned}$$

Here

$$x \equiv \frac{t}{s}, \quad y \equiv \frac{u}{s}, \quad X \equiv \ln\left(-\frac{t}{s}\right), \quad Y \equiv \ln\left(-\frac{u}{s}\right).$$

## References

## Setup

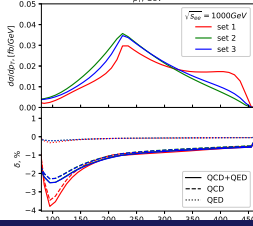
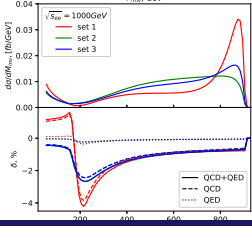
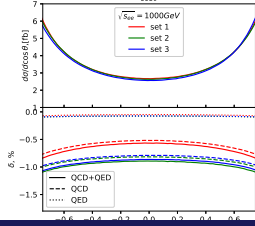
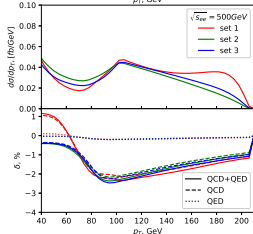
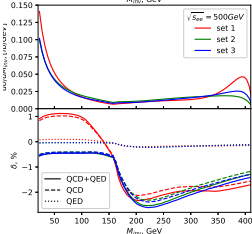
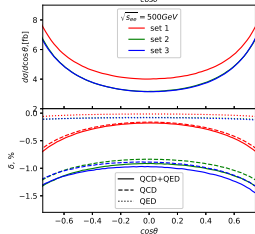
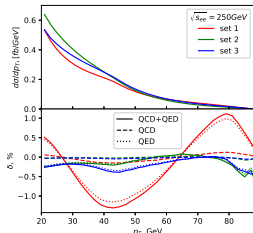
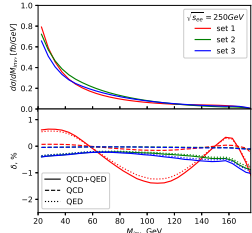
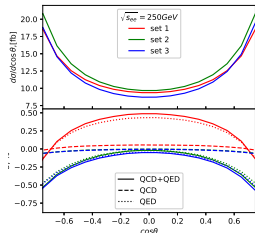
$$\sqrt{s_{ee}} = 250, 500, 1000 \text{ GeV}$$

$$\begin{aligned} \text{set 1 : } & P_e = P'_e = 0.8, \\ & P_\gamma = P'_\gamma = -1, P_t = P'_t = 0, \\ \text{set 2 : } & P_e = P'_e = 0, P_\gamma = P'_\gamma = 0, \\ & P_t = P'_t = 1, \phi = \pi/2, \\ \text{set 3 : } & P_e = 0.8, P'_e = 0, P_\gamma = -1, P'_\gamma = 0, \\ & P_t = 0, P'_t = 1, \phi = \pi/2, \end{aligned} \tag{1}$$

## Results

Integrated one-loop cross sections  $\sigma(\gamma\gamma)$  [fb] and the corresponding relative corrections  $\delta = \sigma_{\text{NLO}}/\sigma_{\text{LO}} - 1$ , [%] for the process  $\gamma\gamma \rightarrow \gamma\gamma$  in different polarization setups

$\sqrt{s_{ee}}$		250 GeV	500 GeV	1 TeV
set 1	$\sigma$ , fb	22.524(1)	9.445(1)	6.940(1)
	$\delta^{\text{QED}}$ , %	0.016(1)	-0.039(3)	-0.062(3)
	$\delta^{\text{QCD}}$ , %	0.125(1)	-0.415(3)	-0.662(3)
set 2	$\sigma$ , fb	24.426(1)	8.045(1)	6.861(1)
	$\delta^{\text{QED}}$ , %	-0.035(2)	-0.099(2)	-0.087(3)
	$\delta^{\text{QCD}}$ , %	-0.278(2)	-1.052(2)	-0.927(2)
set 3	$\sigma$ , fb	22.320(1)	8.014(1)	6.7967(1)
	$\delta^{\text{QED}}$ , %	-0.039(1)	-0.103(2)	-0.084(2)
	$\delta^{\text{QCD}}$ , %	-0.305(2)	-1.101(2)	-0.900(2)





## Conclusion

- The latest version of SANCphot v1.10 has been adapted to study polarized LbL scattering. It incorporates complete electroweak one-loop radiative corrections to realistic observables, as well as massless QCD/QED 2-loop corrections that are relevant for the LbL process.
- The 2-loop QED/QCD corrections make a substantial contribution.
- Another part is expected to emerge from the photon spectrum approximation with the Compton scattering. This question has to be addressed in the further studies.